Using a Josephson junction as an effective on-chip temperature sensor

Using a Josephson junction as an effective on-chip temperature sensor

Paolo Durandetto and Andrea Sosso

INRiM - Istituto Nazionale di Ricerca Metrologica, Strada delle Cacce 91, 10135 Torino, Italy

E-mail: p.durandetto@inrim.it

Abstract. Temperature sensing and control are essential in experiments running in cryocooled systems, as with the case of liquid helium-free superconducting devices. A Josephson junction as on-chip temperature sensor operated in ac provides the highest sensitivity and minimal power loading to the cryogenic environment, thanks to the noise rejection of lock-in detection. To demonstrate the advantages of on-chip sensing, we tested it with a Josephson voltage standard array in cryocooler and compared with the conventional case of a sensor on the cold surface of the refrigerator, showing that the power dissipated within the chip may further increment the device temperature up to some tenths of kelvin. An ac Josephson junction sensor is proven to be capable of directly stabilizing the temperature of the superconductive circuit from fluctuations of dissipated power during operation. Reliability issues related to flux trapping are discussed and solutions are proposed suited to different applications. Overall, on-chip control with ac Josephson temperature sensing has the advantage of avoiding the complexities in minimization of cryogenic thermal links, virtually reducing to zero the contact resistance and keeping the operating temperature of the superconductor constant, independently of instantaneous operating power.

Keywords: Josephson junctions, cryocooler, temperature control, temperature sensor
Submitted to: *Supercond. Sci. Technol.*

1. Introduction

Josephson junctions (JJs) are nowadays massively used as basic blocks in superconductive circuits for a wide range of applications. A prominent example is represented by SQUIDs, extremely sensitive magnetometers that can sense fields for biological studies or measure local magnetic properties of materials. Superconducting tunnel junction detectors represent another instance of application of the unparalleled sensitivity of devices based on the Josephson effect, they may replace CCD devices in cameras with photon-level detection capability. Rapid single flux quantum is a superconductive digital electronic technology to process digital signals, represented by magnetic flux quanta, at orders of magnitude higher in speed and

lower in power consumption with respect to best semiconductor-based solutions. In quantum metrology, Josephson Voltage Standards (JVS) are superconducting integrated circuits with thousands of nearly identical JJs that have been widely investigated by National Metrology Institutes. Taking advantage of the utmost accuracy of Josephson effect in the conversion between frequency and voltage, since frequency can be very accurately determined (e.g. if provided by a caesium clock), they are used in the realization of quantum voltage standards for both constant and time-dependent signals at values up to 20 V [1] and uncertainties as low as 10^{-11} [2].

A major general limitation for a wide application of all superconductive technologies is due to the need of refrigeration at very low temperatures. Although this issue is mitigated when technologies based on high temperature superconductive devices are available [3], operation requires in any case the adoption of sophisticated cryogenics. Liquid He (LHe) temperature is, in any case, the most common requirement for cooling superconductive electronics, considering that niobium, with critical temperature $T_c \simeq 9\,\mathrm{K}$, is used as superconductive material in a large part of devices. However, the increasing shortages and cost of LHe [4] have made the search of alternative cooling methods very intensive. Nowadays, electrically-powered mechanical refrigerators (cryocoolers) are commercially available: these are capable of reaching zero thermal load temperatures below 3 K and cooling powers around 1 W at 4.2 K, which means that heat has to be suitably dissipated to raise the cold stage temperature at the ordinary LHe boiling point. To stabilize the operating temperature, a resistive heater works in tandem with one or more cryogenic temperature sensors, all driven by a controller, usually a commercial instrument with integrated PID (Proportional, Integrative, and Derivative) closed-loop control modes, where the user can set the values for gain (P), reset (I) and rate (D) for optimal response [5] depending on the specific experimental requirements.

To get proper temperature control of the sample under test, heater and sensors should be placed in proximity to the chip and with low thermal resistance links. This is, in most cases, unpractical and the sensors are typically installed onto the cryocooler cold stage (the coldplate, henceforth) or onto the chip carrier, both made with oxygen-free high thermal conductivity (OFHC) copper for maximum uniformity of the temperature in the part. The residual thermal resistance is not low enough in the most demanding conditions and particular care is required in the design of a chip carrier to reduce thermal gradients, mainly at the interfaces between solid bodies. For JVSs working in the high-vacuum environment of a cryocooler, special cryopackages have been designed [6–9], exhibiting thermal resistances between chip and cold heat sink of few kelvin per watt. The case of JVS is particularly interesting and challenging: power levels of some tens of milliwatt are generally dissipated within a JVS, possibly causing its actual temperature to differ from that measured with the the sensor by hundreds of millikelvin. Though JVSs are quantum and, by definition, their behavior is independent on several parameters (temperature, RF power, bias currents, etc.) over a certain range, this temperature offset may be unfavorable or detrimental. Since the offset is unpredictable, the actual device temperature can be significantly higher than the measured one, up to a condition where the value for maximum quantum range is exceeded even if the sensor detects proper operating range.

Therefore, it would be advantageous to directly sense and control the actual chip temperature instead of that of the external sensor, thus reducing the offset in the measurement to a negligible level. JJs for on-chip thermometry have been previously employed to determine the actual chip temperature via the measurement of JJ critical current (I_c) [7, 8, 10]. The novelty here is that the JJ-based sensor is exploited in an automatic chip temperature control system: this has been achieved via the measurement and control of a new electrical parameter, the "apparent" ac resistance of a suitably biased JJ, that can be made extremely sensitive to I_c and, consequently, on temperature. Since, from the practical point of view, the method is very similar to that in use for the widely adopted resistive cryogenic temperature sensors like Cernox®, ruthenium oxide and germanium [11], it can be easily implemented with most commercial instruments, provided that the bias current is user-settable, with clear advantages in terms of simplicity, flexibility and costs. Furthermore, the sensing JJ can be of the same technology of the JJs used in the sample under test, so that the inclusion of a separate junction into the chip structure does not represent a complication for the fabrication process.

2. Methods

Before going into the description of experimental setup, measurements and outcomes, it may be useful to the reader to get familiar with some atypical concepts which are used throughout the paper, such as the "apparent" resistance of a JJ and its sensitivity to temperature changes. Though the experimental work has been carried with ac bias, it is convenient to first introduce the simpler scenario of a dc biased JJ working as temperature sensor.

2.1. Dc-biased JJ sensor

The electrical behavior of a JJ is highly nonlinear, as shown in Figure 1 for the case of an ideal overdamped JJ. Because of nonlinearity, the ratio between voltage and current, namely what we call apparent resistance (R_{JJ}), depends on dc current magnitude I_{dc}: it is zero below I_c and approaches normal resistance R_n for large values. In addition, the current-voltage (IV) characteristic varies with temperature: the critical current I_c always descends with temperature (below T_c), following a relationship that depends on specific junction technology and properties. In the work presented here, the temperature sensitivity of the JJ apparent resistance should be maximized, therefore the bias current has to be set accordingly. The situation of a dc biased JJ subjected to a temperature increase is graphically illustrated in Figure 2, where the effect of ΔT leads to a reduction of I_c (by 10 % in this explanatory example). It is evident that the highest sensor response, i.e. the largest variation of apparent resistance R_{JJ}, is achieved for bias current values in proximity of the critical current I_c.

2.2. Ac-biased JJ sensor: lock-in detection

Although a simple constant bias current is, in principle, sufficient for sensing temperature changes, we adopted an ac bias signal (an option currently available in some high-sensitivity instruments for cryogenic thermometry and thermal control). This allowed us to measure the

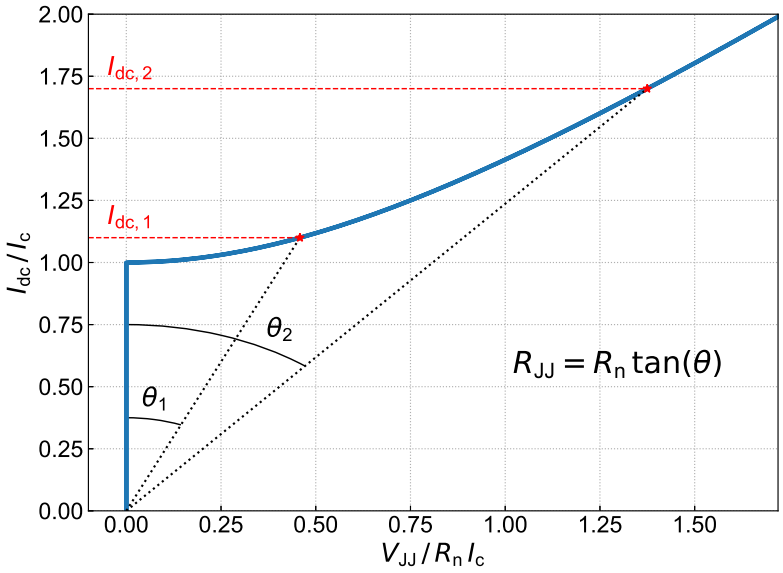

Figure 1. Positive branch of the *IV* characteristic of an ideal overdamped JJ. Current and voltage values are normalized to critical current I_c and normal resistance R_n. The JJ dc apparent resistance is proportional to the tangent of the angle θ, which is related to bias current value I_{dc}.

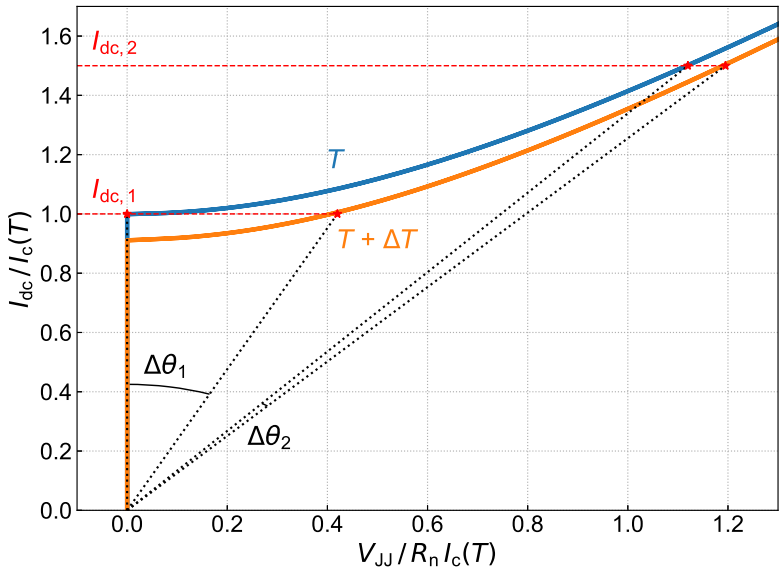

Figure 2. *IV* curves of an ideal overdamped JJ subjected to a temperature increase ΔT. A 10 % reduction of critical current is assumed. Larger $\Delta\theta$ values, and consequently R_{JJ} variations, occur when I_{dc} is close to I_c.

very feeble voltage across the JJ without loss of accuracy by means of lock-in techniques [12], that provide noise rejection at levels unattainable with dc bias. The major difficulty from that choice relies in the study of the electrical model of the nonlinear response of the JJ to a

sinusoidal current excitation. Its complete treatment would be beyond the scope of this paper and will be discussed in a dedicated work.

Some basic knowledge of lock-in operation is necessary for a complete understanding of the discussion in the following, so they are briefly introduced here. The fundamental principle in lock-in detection is reduction of noise, that is generally scattered over a wide frequency band, by selectively filtering out from the input all frequencies but a narrow range around the relevant sinusoidal tone. Such technique can be exploited in all cases where a single tone, constant frequency, test signal can be applied (the reference), so the applications are very wide. Since a linear filter would be unpractical for the high selectivity required, lock-in amplifiers use the homodyne technique, i.e. the multiplication of the input signal per the reference, that generates beat signals with frequencies corresponding to the sum and difference of input and reference frequencies. Sum terms are high in the spectrum and can be removed by a low-pass filter; the frequencies of difference terms increase with the "distance" in frequency of input tones from reference, thus contributions not close to the reference can be removed by a second narrow low-pass filter. The overall effect is then equivalent to very narrowly filtering the input around the reference frequency, with the advantages in noise reduction explained previously. The method is so effective that it can recover signals buried in noise levels that are even six orders of magnitude higher.

In the simple case of an ac current-driven resistor, the time-domain output voltage is a perfect sine wave, i.e. a single tone with amplitude $\tilde{V}$ in the frequency domain. The ac resistance is then given by $\tilde{R} = \tilde{V}/\tilde{I}$, being $\tilde{I}$ the ac current amplitude, and is approximately equal to the dc resistance for low frequency excitation. Instead, the voltage across an ac biased JJ contains several harmonic contributions, of which only the fundamental tone ($\tilde{V}_{\mathrm{JJ}}$) is filtered by the lock-in detector for the determination of the junction ac apparent resistance ($\tilde{R}_{\mathrm{JJ}} = \tilde{V}_{\mathrm{JJ}}/\tilde{I}$). In addition, as with the dc apparent resistance, also $\tilde{R}_{\mathrm{JJ}}$ depends on bias current. However, the analysis is not as straightforward as is in the dc scenario, since the value of the output rms voltage measured by the lock-in depends on the contributions from all instantaneous voltages in the period. Nevertheless, the relationship between ac current amplitude and rms voltage observed with the lock-in detector can be determined, once the *IV* curve is known.

3. Experimental Setup

The setup used in our experiment is very close to the configuration for standard sensor-based operation. It is schematically represented in Figure 3 and the single parts are described in detail hereafter.

3.1. Josephson chip and cryogenic equipment

A programmable Josephson voltage standard (PJVS) with 8192 Superconductor–Normal-metal–Insulator–Superconductor (SNIS) JJs subdivided into fourteen binary-weighted segments [13] was integrated in the cryogenic OFHC Cu carrier described in Reference

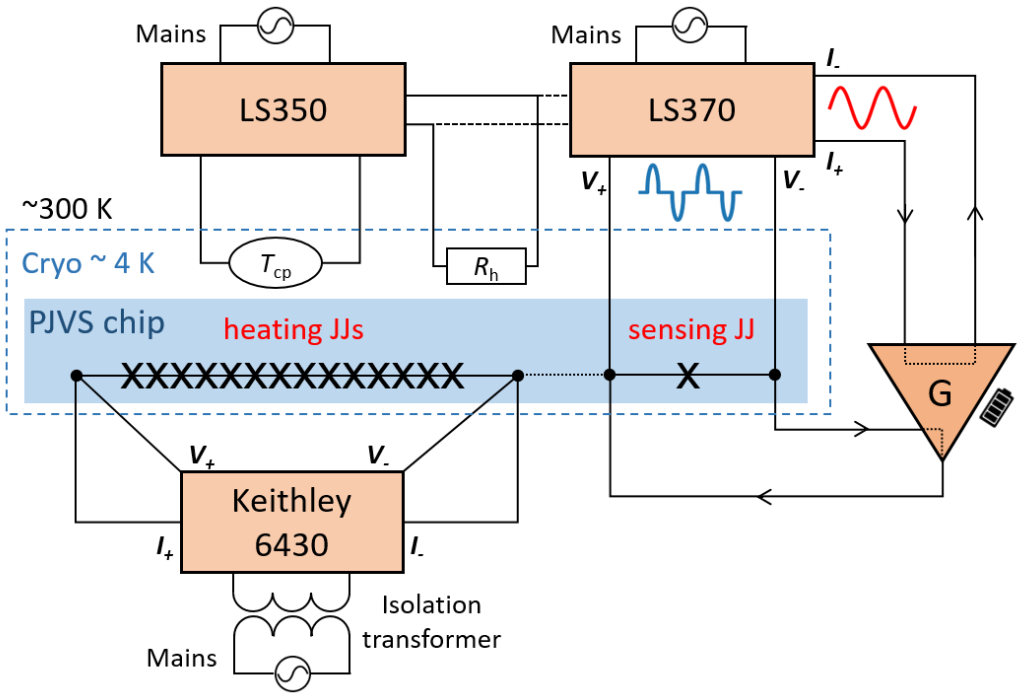

Figure 3. Schematics of the measurement setup. The sensing JJ is connected in a four-wire measurement configuration. The sinusoidal output current (red) from the LS370 is amplified by an adjustable gain-factor G and the resulting voltage across the sensing JJ (blue) is demodulated by the LS370 lock-in circuit. The LS350 controller measured colplate and carrier temperature T_{cp} with two Si diodes (one is shown). The resistive heater R_h is either controlled by LS350 or LS370, depending on the selected reference sensor (Si diode or JJ). The Keithley 6430 sourcemeter provided a four-wire measurement of the heat dissipated by 7936 JJs. The sourcemeter is floating from ground by means of an isolation transformer to avoid interference between simultaneous power and JJ apparent resistance measurements.

[8] and cooled with a two-stage pulse-tube cryocooler (Cryomech PT-410‡), as shown in Figure 4. Two calibrated silicon diode sensors are employed to determine the temperature of cryocooler coldplate and chip carrier, which should be approximately equal as long as these are in good thermal contact. The Si diodes temperature was read with a cryogenic controller, a Lake Shore 350 (LS350, henceforth). Both Cu carrier and coldplate are thermally and electromagnetically shielded in the setup realized for high accuracy measurements for metrology [14]. A manganin wire of resistance $R_h \simeq 80\,\Omega$ at 4.2 K is wound around the coldplate disk as heater, when the temperature is closed-loop controlled.

3.2. Ac electrical resistance bridge and controller

For the determination of the electrical apparent resistance of the sensing JJ we used a commercial ac resistance bridge designed for temperature measurement and control in cryogenics, a Lake Shore 370 (LS370, henceforth). The JJ for temperature sensing is

‡ Brand names are used for identification purposes. Such use implies neither endorsement by INRiM nor assurance that the equipment is the best available

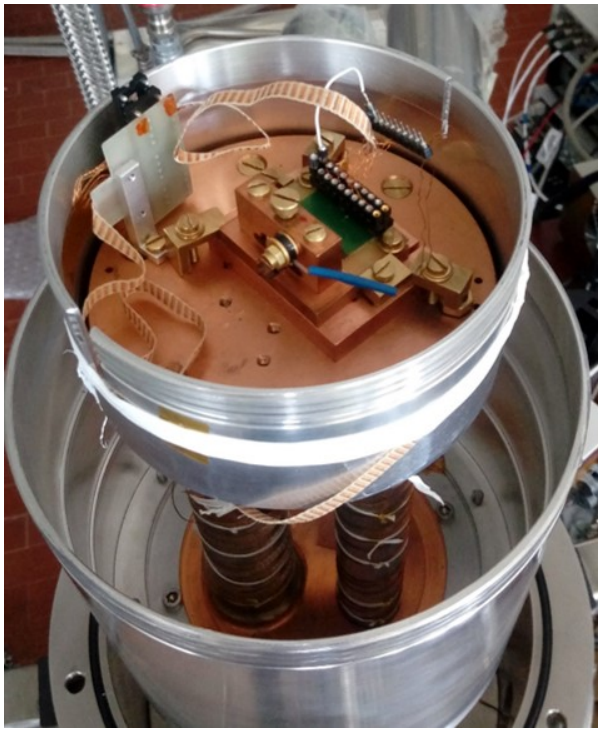

Figure 4. Photograph of the OFHC Cu carrier containing the PJVS device, mounted onto the coldplate of the pulse-tube cryocooler.

connected in the four-wire configuration usually adopted in accurate resistance measurement. Despite the name, LS370 is not a true resistance bridge: as stated in the operation manual [15], it *does not use a bridge configuration for resistance measurement [...]. The name "Bridge" was retained to reflect the instrument's heritage of precision resistance measurements*. Its measurement principle relies on the lock-in detection of the output voltage across an ac current-biased sensor (see Sec. 2.2). Indeed, ac controllers are designed to accurately measure the temperature-dependent electrical resistance of cryogenic sensors. In typical conditions, current excitation and resistance range are properly chosen to simultaneously maintain acceptable accuracy and resolution and avoid large heat generation into the sensor. The output current is then in general very low and, for the LS370, is selectable between twenty-one logarithmically-spaced current levels with rms values ranging from 3.16 pA to 31.6 mA, whereas the reference frequency can be chosen among 9.8, 13.7 and 16.2 Hz. At such low frequencies, parasitic capacitance and skin effect are negligible, and, for a purely resistive element, ac resistance is equal to dc resistance.

3.3. Variable-gain current amplifier

To override a limitation of the LS370, that allows to regulate the ac bias current only in finite increments, we added a custom designed current amplifier at its output to vary continuously the current within the step-to-step intervals. That makes it possible to finely set the JJ bias for maximum temperature sensitivity. The value of the amplified current flowing through the JJ

is determined by means of a shunt resistance and a battery-operated voltmeter. At this point, we have to clarify that the resistance value displayed by the LS370 is systematically higher than the real one by a factor equal to the amplifier gain (G), in that the pre-amplified current value is used in the resistance calculation by the instrument firmware. However, this "fake" resistance is considered as a setpoint reference for controlling the temperature and may be regarded as a temperature dependent parameter with no physical meaning.

3.4. On-chip heat source

To quantify the Joule heat dissipated inside the device and the effectiveness of on-chip sensing, a high-accuracy current source is used to bias the five larger sections of the PJVS array above the critical current. Since these sections include 7936 series-connected JJs, values of the total voltage up to 5 V are generated with dissipated power (P_d) in the range 0–100 mW. A Keithley 6430 sourcemeter both provided dc current and measured the resulting voltage drop and, hence, P_d. Four terminal connection allows to accurately measure the total voltage of the series and determine the dissipated electrical power with accuracy around 1 %. An isolation transformer was inserted between mains power and sourcemeter, with the aim of electrically decoupling the latter from ground and, hence, avoiding interference in the $\tilde{R}_\mathrm{JJ}$ measurement.

4. Measurements and results

4.1. Characterization of the sensing JJ

The *IV* curves of the sensing JJ have been recorded at temperatures from 3.8 K to 4.6 K, with the operating temperature stabilized in the conventional way, i.e. through the PID feedback control of the LS350 controller with a Si-diode as temperature sensor and the resistive heater as power source. No temperature differences between the diodes were ever observed, meaning that the thermal resistance between carrier and coldplate is negligible and that these were in thermal equilibrium. Additionally, the low power (always below 0.5 mW) generated inside the chip by test signals, jointly with a value of the chip-to-carrier thermal resistance of a few $\mathrm{K\,W^{-1}}$ (see Sec. 4.3) guarantee that the difference in temperature from chip to carrier is, in the worst case, of the order of a few mK and can be neglected. Both chip and carrier were then considered isothermal during this characterization.

From these *IV* curves, we obtained the pointwise input/output relationship that allowed us calculate the JJ voltage waveform in one period, i.e. the signal at the lock-in input. Finally, taking the rms amplitude of the fundamental tone in the Fast Fourier Transform (FFT) of this signal, we processed data analogously to what is done in the firmware, obtaining the lock-in output rms value and the ac apparent resistance given by the instrument.

4.2. Measurement of JJ ac apparent resistance vs. temperature

The JJ ac apparent resistance $\tilde{R}_\mathrm{JJ}$ has been then measured over the same range of temperatures for different ac current amplitudes. The operating temperature T_cp was again stabilized with

the LS350 controller, diode sensor and heater, providing the same experimental conditions as in previous test, from the point of view of thermal environment.

Experimental results are summarized in Figure 5, along with the $\tilde{R}_{JJ}$ values determined with numerical calculations from the previously recorded *IV* curves. It can be seen that the Fourier analysis model adequately describes the real JJ behavior, especially for bias current values close to $I_c(T_{cp})$. It can also be argued that the $\tilde{R}_{JJ}$ sensitivity to temperature changes is accentuated for ac bias close to the critical current value at the temperature to be stabilized.

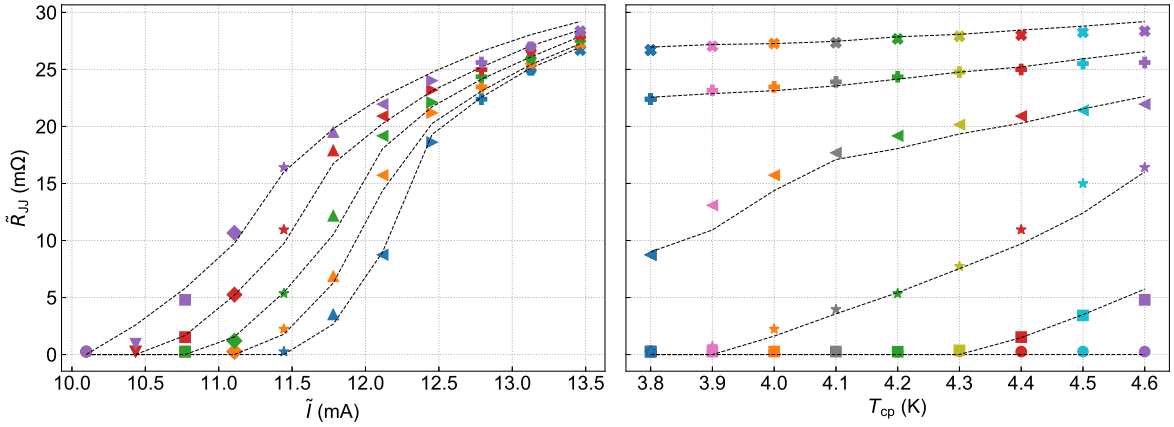

Figure 5. Ac apparent resistance $\tilde{R}_{JJ}$ of the sensing JJ as a function of bias current amplitude $\tilde{I}$ (left) and coldplate-cryopackage temperature T_{cp} (right). Same-color data were taken at equal temperature T_{cp}, whereas same-marker data were recorded with equal ac bias current $\tilde{I}$. Black-dashed lines represent the trends derived from numerical analysis of previously recorded *IV* curves.

4.3. Temperature and JJ ac apparent resistance control under heat generation

In the second part of the experiment, the temperature measured by the diodes and the JJ ac apparent resistance were alternately controlled via the PID closed-loop function of the two commercial instruments. The setpoint temperature was 4.2 K. To enhance temperature sensitivity, the JJ was current-driven slightly above the critical current at 4.2 K, namely at 11.3 mA, where $\tilde{R}_{JJ} \simeq 2\,\text{m}\Omega$ is observed. Thermal power up to 100 mW was then dissipated through the 7936 JJs array and measured with the sourcemeter, thus simulating the heat generated by a both dc and RF biased quantum voltage standard.

Observing Figure 6, it can be seen that, when the temperature of the coldplate-carrier system is regulated by the LS350 through the diode, $\tilde{R}_{JJ}$ increases up to 10 mΩ (almost five-fold) at 100 mW, as a consequence of the non-null chip-to-carrier thermal resistance. From the left plot of Figure 5 and for $\tilde{I} \simeq 11.3\,\text{mA}$, an $\tilde{R}_{JJ}$ of approximately 10 mΩ is observed around 4.5 K (about halfway between purple-diamond and red-star markers), from which the package thermal resistance at $T_{cp} \simeq 4.2\,\text{K}$ is determined as $(T_{JJ} - T_{cp})/P_d = 0.3\,\text{K}/0.1\,\text{W} = 3\,\text{K}\,\text{W}^{-1}$. Vice versa, the actual chip temperature can be directly sensed and controlled by stabilizing $\tilde{R}_{JJ}$ with the LS370 ac meter/controller, as demonstrated in the bottom plot of Figure 6. This results in the lowering of the cryocooler base temperature T_{cp}, such that the "temperature

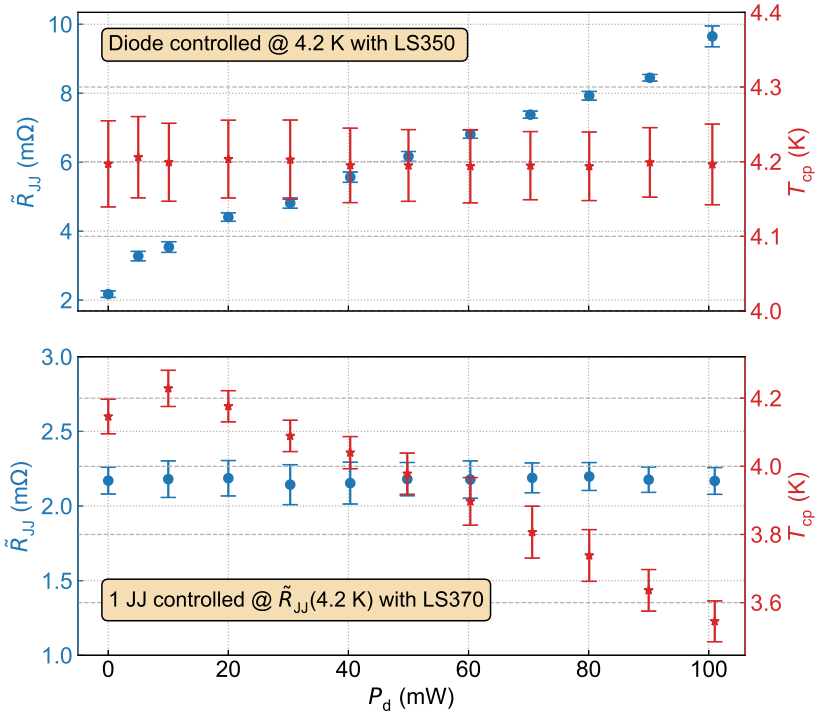

Figure 6. Sensing JJ apparent resistance $\tilde{R}_{JJ}$ and coldplate-carrier temperature T_{cp} for different values of the power P_d dissipated by the 7936 JJs segment. Top: the coldplate-carrier temperature T_{cp} was controlled with the LS350 PID function. Bottom: the ac apparent resistance $\tilde{R}_{JJ}$ of the sensing JJ was controlled with the LS370 PID function.

drop" caused by the dissipated power flowing through a non-zero thermal resistance is compensated, thus keeping the chip at a constant temperature. In the electrical analogy of a dc current-driven resistor, this is like the voltage at the low potential side is regulated to maintain the high potential side at a fixed absolute voltage. In our experiment, the coldplate-carrier temperature T_{cp} decreased down to about 3.6 K at 100 mW: the overall thermal resistance calculation would then give $(T_{JJ} - T_{cp})/P_d = (4.2\,\mathrm{K} - 3.6\,\mathrm{K})/0.1\,\mathrm{W} \simeq 6\,\mathrm{K\,W^{-1}}$, which is doubled compared to the previous case because both cryocooler and cryopackage thermal resistances increase at lower temperature. Being the cooling power of the cryocooler in use approximately equal to 500 mW at 3.6 K [16], an average power around 400 mW is provided by the feedback loop circuit through the resistive heater R_h. Therefore, on-chip power dissipation exceeding 100 mW and simultaneous chip temperature stabilization at 4.2 K are possible through the controlled reduction of the Joule heat from R_h. Alternatively, more relaxed requirements in terms of refrigerator cooling capacity and/or cryopackage thermal conductance have to be met in case of lower on-chip power values.

5. Conclusions

We analyzed how to exploit the sensitivity of a Josephson junction to temperature for directly sensing the temperature of a superconductive chip, and the improvements that can be achieved in superconductive electronics applications. For several reasons the sensor signals must be kept as low as possible, thus, even if a dc sensing signal would be feasible, ac signals are necessary to provide adequate sensitivity via lock-in detection.

By means of a setup modified for the purpose, we were able to characterize a JJ as sensor operated in ac. Starting from the *IV* curve recorded over a selected range of temperatures around 4.2 K, the voltage across the JJ biased with a sinusoidal current was calculated from the nonlinear JJ response as a function of temperature and bias amplitude, then the harmonic component at the bias frequency was extracted to determine the rms amplitude as observed by a lock-in detector. From the ratio of rms voltage and current, the ac apparent resistance of the JJ was finally determined as in the experiment. Eventually, the comparison with the ac apparent resistance measured in the experiment confirmed the calculated values, proving that the behavior of the JJ temperature sensor in ac regime is fully calculable. This can be used, for instance, to optimize JJ parameters and operating conditions, e.g maximizing measurement sensitivity.

To demonstrate the advantages of high sensitivity ac on-chip sensing, the particular case of He-free cooled devices was considered, where the control of operating temperature is mandatory and more practical than in a He bath. By comparing the chip temperature with the temperature of the high thermal conductivity chip carrier, we were able to calculate a residual chip-to-carrier thermal resistance of about $3\,\mathrm{K\,W^{-1}}$ rising the temperature of the chip up to 0.3 K in a worst case experimental condition of 100 mW dissipation. On the other hand, the direct stabilization of chip temperature by replacing the conventional sensor with a JJ was shown to be feasible with minimal modifications of the setup. This solution has the relevant advantage of avoiding all issues related to the optimization of the thermal link from chip to the cooler cold surface, which is known to be complex and limited by the low conductance of the interfaces between different parts. A feedback loop driven by the temperature measured on chip completely overcomes the problems, by automatically reducing the coldplate temperature to compensate the increase for chip power dissipation, virtually multiplying the physical thermal conductance by a factor equal to the loop gain.

Finally, it can be quite easily overcome the well known proneness of niobium, and more generally type II superconductive materials, to flux trapping [17], consequently this is not a limiting factor in practical usage of the JJ temperature sensor described. First, it should be considered that temperature measurement are here considered as relative: since it is difficult in practice to guarantee that I_c is not reduced by trapped flux, a defined I_c value is not related to a precise temperature. Rather, one must consider that the knowledge of absolute temperature is not essential for the operation of superconductive devices, since their temperature-dependent behavior changes significantly with the fabrication process parameters. Thus, in practice, the operating temperature is set by the expected behavior (e.g. a certain value of I_c) and the task of the temperature control is to keep the temperature constant to that value, as done by the JJ

sensor. Possible issues from a sudden change in trapped flux are also ruled out, in that these induce a discontinuous effect, detectable if relevant, in the behavior of the device under test. In any case, with proper shielding, flux trapping during the experiment were seldom observed and, if reliability is mandatory, sensor redundancy can be easily implemented. To summarize, a JJ on-chip temperature sensor provides in general an effective solution for local temperature monitoring and control of superconductive electronics.

References

[1] Müller F, Scheller T, Wendisch R, Behr R, Kieler O, Palafox L and Kohlmann J 2013 *IEEE Transactions on Applied Superconductivity* **23** 1101005–1101005

[2] Solve S, Rüfenacht A, Burroughs C J and Benz S P 2013 *Metrologia* **50** 441–451 URL https://doi.org/10.1088%2F0026-1394%2F50%2F5%2F441

[3] Seidel P (ed) 2015 *Applied superconductivity: handbook on devices and applications* (John Wiley & Sons)

[4] Kramer D 2019 *Phys. Today* **72** 26–29 URL https://physicstoday.scitation.org/doi/10.1063/PT.3.4181

[5] Swartz J M and Rubin L G Fundamentals for usage of cryogenic temperature controllers Lake Shore Cryotronics Application Note

[6] Schwall R E, Zilz D P, Power J, Burroughs C J, Dresselhaus P D and Benz S P 2011 *IEEE Trans. Appl. Supercond.* **21** 891–895

[7] Schubert M, Starkloff M, Peiselt K, Anders S, Knipper R, Lee J, Behr R, Palafox L, Böck A C, Schaidhammer L *et al.* 2016 *Supercond. Sci. Technol.* **29** 105014

[8] Durandetto P, Monticone E, Serazio D and Sosso A 2019 *IEEE Trans. Compon. Packag. Manuf. Technol.* **9** 1264–1270

[9] Yamamori H, Maruyama M, Amagai Y and Shimazaki T 2019 *IEICE Electronics Express* 16–20190219

[10] Fox A E, Golden E B, Dresselhaus P D and Benz S P 2017 *IEEE Transactions on Applied Superconductivity* **27** 1–5

[11] Lake Shore Cryotronics 2019 Cryogenic temperature sensors URL https://www.lakeshore.com/products/categories/temperature-products/cryogenic-temperature-sensors

[12] Meade M L 1983 *Lock-in amplifiers: principles and applications* IEE electrical measurement series (P. Peregrinus (on behalf of IEE))

[13] Lacquaniti V, De Leo N, Fretto M, Sosso A, Müller F and Kohlmann J 2011 *Supercond. Sci. Technol.* **24** 045004

[14] Sosso A, Fretto M, Lacquaniti V, Monticone E, Rocci R, Serazio D and Trinchera B 2015 *Journal of Supercond. and Novel Magnetism* **28** 1181–1184

[15] Lake Shore Cryotronics 2009 *User's Manual Model 370 AC Resistance Bridge* URL https://www.lakeshore.com/docs/default-source/product-downloads/manuals/370

[16] Cryomech PT410 Cryorefrigerator Capacity Curve URL https://www.cryomech.com/wp-content/uploads/2018/11/PT410_cc.pdf

[17] Fulton A, Hebard A, Dunkleberger L and RH E 1977 *Solid State Commun.* **22** 493–496